LETTERS
PUBLISHED ONLINE: 14 FEBRUARY 2010 | DOI: 10.1038/NPHOTON.2010.3

nature photonics

Exploiting disorder for perfect focusing

I. M. Vellekoop[1†], A. Lagendijk[2] and A. P. Mosk[1*]

Optical microscopy and manipulation methods rely on the ability to focus light to a small volume. However, in inhomogeneous media such as biological tissue, light is scattered out of the focusing beam. Disordered scattering is thought to fundamentally limit the resolution and penetration depth of optical methods[1-3]. Here we demonstrate, in an optical experiment, that scattering can be used to improve, rather than deteriorate, the sharpness of the focus. The resulting focus is even sharper than that in a transparent medium. By using scattering in the medium behind a lens, light was focused to a spot ten times smaller than the diffraction limit of that lens. Our method is the optical equivalent of highly successful methods for improving the resolution and communication bandwidth of ultrasound, radio waves and microwaves[4-6]. Our results, obtained using spatial wavefront shaping, apply to all coherent methods for focusing through scattering matter, including phase conjugation[7] and time-reversal[4].

The initial configuration of the experiment is shown in Fig. 1a. A lens focuses a beam of light onto a charge coupled device (CCD) camera. In this 'clean' system without disorder, the sharpness of the focus is limited by the numerical aperture and the quality of the lens. The light propagation is now disturbed by placing a non-transparent scattering object in the beam path. Although the focus initially disappears, it can be restored by shaping the wavefront of the incident light using a spatial light modulator[8,9] (see Fig. 1b). An intriguing quality of the restored focus is now reported and analysed. The experimentally obtained focal spot is smaller than the diffraction limit of the clean system. We show both experimentally and theoretically that it is the scattering medium, rather than the lens or the quality of the reconstruction process, that determines the width of the focus, a surprising property of scattered light that is in line with observations in ultrasound experiments[4,10].

In Fig. 2a we show the measured intensity distribution in the focal plane of the clean system. Ideally, the lens would focus light to an Airy disk of width $w = 1.03\lambda f_1/D_1$, where w is the full-width at half-maximum (FWHM). In our experiment, $\lambda = 632.8$ nm, $f_1 = 200$ mm and $D_1 = 2.1$ mm, which gives a diffraction limited spot size of 62 μm. In reality, the focus has a slightly larger width of 76 ± 3 μm.

When the beam path is blocked by a disordered medium (a 6-μm layer of opaque white airbrush paint), the image on the camera changes dramatically. Instead of a focus, a disordered speckle pattern is recorded (Fig. 2b). Typically, the light is scattered and diffracted about a hundred times before reaching the other side of the sample. Therefore, the transmitted wave has lost all correlation with the incident wavefront[11], and the efficient wavefront correction systems that have been developed in adaptive optics cannot be used[12]. The focus is recovered using an approach that was designed specifically for strongly scattering environments. A spatial light modulator shapes the wavefront of the light that impinges on the lens. The surface area of the light modulator is subdivided into 64×64 square segments, which are phase-modulated[13] and controlled by a learning feedback algorithm (see Supplementary Methods). The surface of the modulator is imaged onto the central plane of the lens. The algorithm adjusts the relative phases of the segments so that the transmitted light interferes constructively in a chosen target, thereby creating a focus at that point. In this case, the target was formed by a single 6.45 μm × 6.45 μm CCD pixel in the centre of the desired focus. The algorithm finds the optimal wavefront for focusing on this target (Fig. 2d). The optimal wavefront is completely disordered, which confirms that the sample is strongly scattering.

Figure 2c presents the intensity distribution after running the algorithm. The scattered light now focuses to a tight spot, even though the algorithm did not optimize the shape of the focus explicitly. What is more, the width of this spot is approximately one tenth of the diffraction limit of the lens. In other words, scattering has greatly improved the focusing resolution.

To analyse this striking effect, we placed the sample at different distances f_2 from the camera. Figure 3 illustrates the width of the focus in these experiments. The widths decrease as the sample is moved closer to the camera, and are always smaller than the width of the diffraction

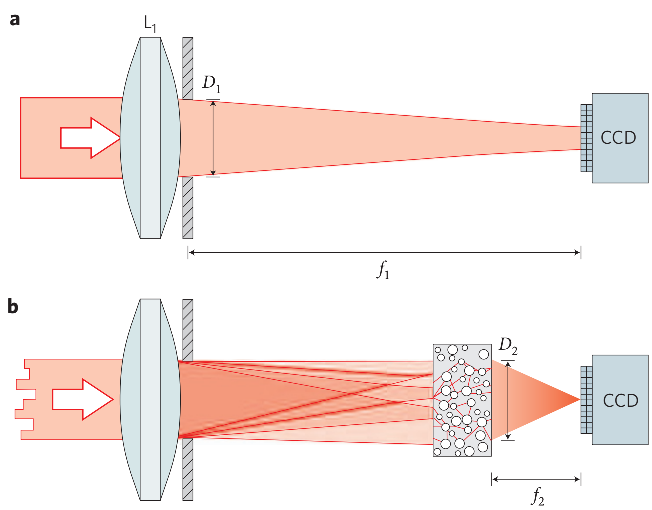

Figure 1 | Schematic of the experiment. Lens L_1 with focal distance f_1 focuses light onto a camera. A pinhole controls the aperture D_1 of the lens. **a**, 'Clean' system without disorder. The focus is, at best, as sharp as the diffraction limit of the lens. **b**, System with disorder. A disordered sample at distance f_2 from the camera randomly scatters the light. After shaping the incident wavefront with a spatial light modulator (modulator and imaging telescope not shown), the light focuses through the sample to a spot that is narrower than the diffraction limit. D_2, diameter of the diffuse spot at the back of the sample.

[1]Complex Photonic Systems, Faculty of Science and Technology, and MESA+ Institute for Nanotechnology, University of Twente, PO Box 217, 7500 AE Enschede, The Netherlands, [2]FOM Institute for Atomic and Molecular Physics, PO Box 41883, 1009 DB Amsterdam, The Netherlands; †Present address: Physik Institut, University of Zurich, Winterthurerstrasse 190, CH-8057 Zurich, Switzerland. *e-mail: a.p.mosk@utwente.nl

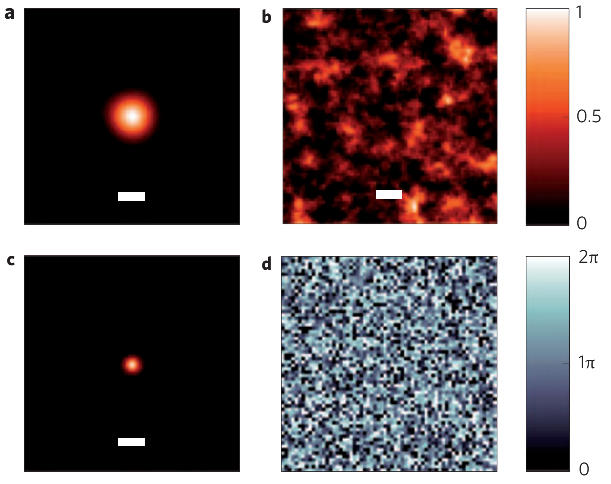

Figure 2 | Measured intensity distribution in the focal plane at 200 ± 3 mm from the glass lens. a, Clean system with an unmodified incident wavefront. The focal width is of the order of the diffraction limit (62 μm, white bar). **b**, Intensity transmission of a 6-μm layer of airbrush paint for the unmodified incident wavefront. No focus is discernible. **c**, System with the sample present, and the wave shaped to achieve constructive interference in the target. A high-contrast, extremely sharp focus is visible. **d**, Pattern on the spatial phase modulator for the set-up in **c**. The intensity plots are normalized to the brightest point in the image.

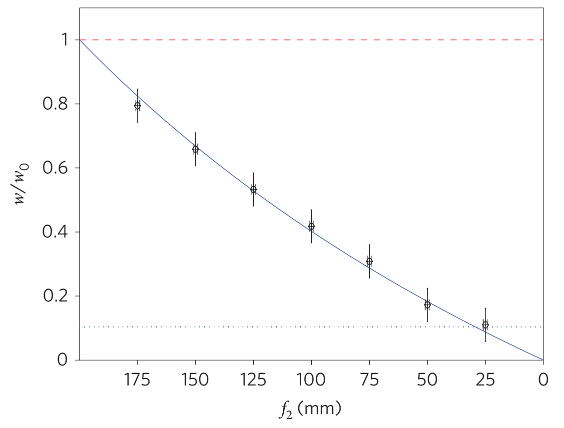

Figure 3 | Focal width w, relative to the diffraction limit of the glass lens (w_0 = 62 μm, dashed line), as a function of the distance f_2 between the scattering sample and the focal plane. Diamonds indicate measured values with a sample present. The solid curve indicates the theoretical effective diffraction limit (no free parameters) and the dotted line, the size of a single pixel of the camera.

limited spot of the clean system. At distances of 25 mm or less, the width of the focus is smaller than a single camera pixel, almost a factor of ten below the diffraction limit of the lens.

We will now quantitatively define an effective diffraction limit for a scattering system and show that the width of the smallest achievable focus is given by the FWHM of an Airy disk,

$$w = 1.03\lambda f_2/D_2 \tag{1}$$

where f_2 is the distance between the scattering layer and the focal plane and D_2 is the diameter of the illuminated area on the scattering layer.

Figure 3 plots the theoretical effective diffraction limit as a function of the distance between the scattering layer and the focal plane, f_2. The theoretical limit decreases almost linearly as the sample is moved closer to the chosen focus. With no adjustable parameters, the experimentally observed focal widths equal the theoretical lower limit predicted by the model.

To understand why the scattered light focuses to exactly the theoretically smallest possible focus — even though no effort is made to explicitly minimize the width of the focus — we now calculate how a shaped wavefront propagates through a scattering sample. The propagation of light from a source at $\mathbf{r}_\alpha$ to a target at $\mathbf{r}_\beta$ through a sample is described by the stochastic Green function $G(\mathbf{r}_\beta, \mathbf{r}_\alpha)$. Theoretically[14,15], the maximum intensity transmission is achieved when the incident field $E(\mathbf{r}_\alpha)$ is modulated spatially so that $E(\mathbf{r}_\alpha) \propto G^*(\mathbf{r}_\beta, \mathbf{r}_\alpha)$, where * denotes the complex conjugate. Our algorithm constructs this wavefront by maximizing the intensity at point $\mathbf{r}_\beta$. This is the same wavefront that one would get when one would phase conjugate the light[7] coming from a (hypothetical) source at $\mathbf{r}_\beta$.

If all channels on both sides of the sample could be controlled, the light would form a perfect spherical wave[14] that converges to point $\mathbf{r}_\beta$. In a transmission geometry, only a finite number of channels on one side of the sample are controlled. Therefore it is, even in principle, impossible to perfectly focus all incident light. However, because the sample completely scrambles the incident wavefront, any deviation from the perfect wave is randomly distributed over all outgoing angles. Therefore, the average field at the back of the sample still constitutes a converging spherical wave originating from the illuminated part of the sample (see also Supplementary Equations),

$$\langle E(\mathbf{r}_k; \mathbf{r}_\beta)\rangle = g^*(\mathbf{r}_\beta - \mathbf{r}_k)C_0 I_0(\mathbf{r}_k) \tag{2}$$

where $E(\mathbf{r}_k; \mathbf{r}_\beta)$ denotes the field at point $\mathbf{r}_k$ on the back of the sample after programming the modulator to optimize the intensity in target $\mathbf{r}_\beta$ and $\langle\cdot\rangle$ is the ensemble averaging operator. g is the Green function for propagating through air, C_0 is a constant to normalize the total incident power, and $I_0(\mathbf{r}_k)$ is the ensemble averaged intensity distribution at the back of the sample. Equation (2) shows that experimental limitations do not change the shape of the focus; they merely cause the contrast with the speckle background to decrease[10].

The term $I_0(\mathbf{r}_k)$ in equation (2) acts as an effective aperture function for the scattering 'lens'. In our experiments $I_0(\mathbf{r}_k)$ is approximated well by a top hat disk with a diameter of D_2. In this case, equation (2) describes diffraction limited focusing at point $\mathbf{r}_\beta$ by a lens with a clear aperture of D_2. This result explains the experimental observation in Fig. 3 that the focal width always equals the theoretical minimum.

The intensity distribution in the focal plane is found from equation (2) by paraxially propagating the field. In the Supplementary Equations we derive

$$I(\mathbf{r}_b; \mathbf{r}_\beta) = S_I|\mathcal{F}\{I_0(\mathbf{r}_k)\}|^2 \tag{3}$$

where $\mathcal{F}\{\}$ is the two-dimensional Fourier transform, S_I is a normalization constant that is fixed by the condition that $I(\mathbf{r}_\beta; \mathbf{r}_\beta) = I_0(\mathbf{r}_\beta)(\pi(N-1)/4 + 1)$, with N being the number of independent modulator segments and I_0 the average intensity of the diffuse background before optimization[8,15]. The intensity in the focus increases linearly with the number of segments, until N is equal to the total number of degrees of freedom of the optical field.

Equation (3) predicts the shape of the reconstructed focus. Surprisingly, this equation takes the same form as the van Cittert–Zernike theorem[16]. This theorem tells us that the speckle correlation function is proportional to $|\mathcal{F}\{I_0(\mathbf{r}_k)\}|^2$. Our derivations suggest an alternative interpretation of this decades-old theorem: the theorem predicts the exact shape to which a disordered sample will focus an optimized wavefront.

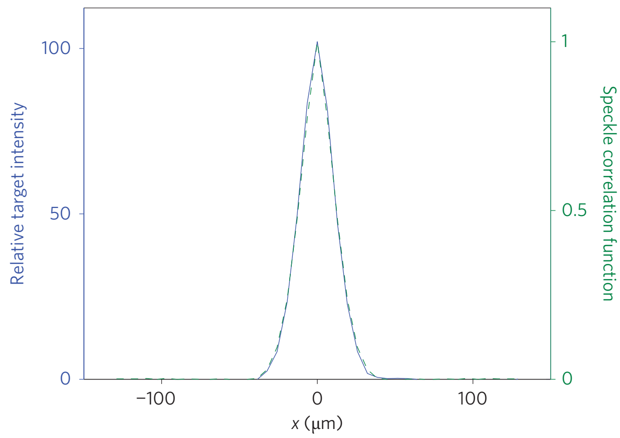

Figure 4 | Intensity profile of the focus at $y = 0$ (solid curve) and speckle correlation function (dashed curve). Results for a 6-μm-thick layer of airbrush paint creating a focus at a distance of 10.0 cm. The speckle correlation function was measured with a randomly generated incident wavefront.

To test this remarkable result, we compared the measured shape of the reconstructed focus to the measured autocorrelate of the background speckle. In Fig. 4, the two normalized curves can be seen to overlap perfectly. We repeated this experiment in different geometries and with different samples and found that the shape of the focus is always in agreement with the shape that the van Cittert–Zernike theorem predicts.

In conclusion, scattering in a medium behind a lens can be used to improve the focusing resolution to beyond the diffraction limit of that lens. Because the position of the focus can be chosen, the disordered system even acts as a zoom lens. We found that, surprisingly, the shape of the focus is not affected by experimental limitations of the wavefront modulator: the focus is always exactly as sharp as is theoretically possible.

Disordered scattering has been applied to improve resolution and bandwidth in imaging and communication with ultrasound, radio waves and microwaves[4–6], and significant sub-wavelength effects have been demonstrated[17]. Our results are the first demonstration that similar resolution improvements can be obtained in photonics. Calculations[18,19] indicate that useful optical superresolution will be achieved using our method on plasmonic nanostructures. We anticipate that disorder-assisted focusing, combined with a method for scanning the focus[9], will lead to improvements in the imaging resolution of microscopy in inhomogeneous media.

Received 16 August 2009; accepted 8 January 2010; published online 14 February 2010

References

1. Ishimaru, A. *Wave Propagation and Scattering in Random Media* (Academic Press, 1978).
2. Sebbah, P. (ed.) *Waves and Imaging through Complex Media* (Kluwer Academic, 2001).
3. Hayakawa, C. K., Venugopalan, V., Krishnamachari, V. V. & Potma, E. O. Amplitude and phase of tightly focused laser beams in turbid media. *Phys. Rev. Lett.* **103,** 043903 (2009).
4. Derode, A., Roux, P. & Fink, M. Robust acoustic time reversal with high-order multiple scattering. *Phys. Rev. Lett.* **75,** 4206–4209 (1995).
5. Foschini, G. J. Layered space–time architecture for wireless communication in a fading environment when using multi-element antennas. *Bell Labs Tech. J.* **1,** 41–59 (1996).
6. Simon, S. H., Moustakas, A. L., Stoytchev, M. & Safar, H. Communication in a disordered world. *Phys. Today* **54,** 38–43 (2001).
7. Yaqoob, Z., Psaltis, D., Feld, M. S. & Yang, C. Optical phase conjugation for turbidity suppression in biological samples. *Nature Photon.* **2,** 110–115 (2008).
8. Vellekoop, I. M. & Mosk, A. P. Focusing coherent light through opaque strongly scattering media. *Opt. Lett.* **32,** 2309–2311 (2007).
9. Popoff, S. M. *et al.* Measuring the transmission matrix in optics: an approach to the study and control of light propagation in disordered media. Preprint at <http://ArXiv: physics.optics/0910.5436v1> (2009).
10. Derode, A., Tourin, A. & Fink, M. Random multiple scattering of ultrasound. II. Is time reversal a self-averaging process? *Phys. Rev. E* **64,** 036606 (2001).
11. Pappu, R., Recht, B., Taylor, J. & Gershenfeld, N. Physical one-way functions. *Science* **297,** 2026–2030 (2002).
12. Tyson, R. K. *Principles of Adaptive Optics* 2nd edn (Academic Press, 1998).
13. van Putten, E. G., Vellekoop, I. M. & Mosk, A. P. Spatial amplitude and phase modulation using commercial twisted nematic LCDs. *Appl. Opt.* **47,** 2076–2081 (2008).
14. Tanter, M., Thomas, J.-L. & Fink, M. Time reversal and the inverse filter. *J. Acoust. Soc. Am.* **108,** 223–234 (2000).
15. Vellekoop, I. M. & Mosk, A. P. Universal optimal transmission of light through disordered materials. *Phys. Rev. Lett.* **101,** 120601 (2008).
16. Goodman, J. W. *Statistical Optics* (Wiley, 2000).
17. Lerosey, G., de Rosny, J., Tourin, A. & Fink, M. Focusing beyond the diffraction limit with far-field time reversal. *Science* **315,** 1120–1122 (2007).
18. Stockman, M. I., Faleev, S. V. & Bergman, D. J. Coherent control of femtosecond energy localization in nanosystems. *Phys. Rev. Lett.* **88,** 067402 (2002).
19. Bartal, G., Lerosey, G. & Zhang, X. Subwavelength dynamic focusing in plasmonic nanostructures using time reversal. *Phys. Rev. B* **79,** 201103 (2009).

Acknowledgements

The authors thank W.L. Vos and E.G. van Putten for support and discussions. This work is part of the research programme of the Stichting voor Fundamenteel Onderzoek der Materie (FOM), which is financially supported by the Nederlandse Organisatie voor Wetenschappelijk Onderzoek (NWO). A.P.M. is supported by a VIDI grant from NWO.

Author contributions

I.M.V., A.L. and A.P.M. designed the experiments, analysed the data, developed the theory and wrote the paper. I.M.V. performed the experiments.

Additional information

The authors declare no competing financial interests. Supplementary information accompanies this paper at www.nature.com/naturephotonics. Reprints and permission information is available online at http://npg.nature.com/reprintsandpermissions/. Correspondence and requests for materials should be addressed to A.P.M.